



SHEAR STRENGTH AND DEFORMATION CAPACITY MODELS FOR RC COLUMNS

Mehrdad SASANI¹

SUMMARY

Experimental test results of 89 reinforced concrete (RC) columns and shear force transfer mechanics are used to develop a new shear strength capacity model for RC columns. The model accounts for the effects of the aspect ratio (shear span divided by the depth of section), compressive load, and displacement ductility on the shear strength capacity. It is shown that compared to available models in current codes and standards, the proposed model predicts more reliably the shear strength of columns. The coefficient of variation of the new model is only 0.14.

Based on the mechanics of deformation of columns and using the experimental test results a new drift ratio capacity model is also proposed. In addition to the effects of the transverse reinforcement, axial load, and aspect ratio, the difference between the deformation of double curvature and double ended columns (in which damage can concentrate on one end of the specimen) and cantilever columns is accounted for. The coefficient of variation of the drift capacity model is 0.22.

INTRODUCTION

In design of new structures, it is well recognized that the designer must try to avoid any brittle modes of local, story or global failure and let the overall structural behavior be mainly controlled by ductile and tough modes. In seismic assessment of existing RC structures it is important to predict any brittle type of behavior and the possibility of such failure of columns subjected to shear, axial, and flexural load is perhaps the most important one that needs to be examined. It is important not only to look at the behavior of a single column under high shear forces, but also to study the effects of such a behavior on the structure as a whole. For instance, at the near-collapse seismic performance level, there is a need to predict and model the reduction in the lateral load carrying capacity of shear sensitive columns, their possible loss of axial load carrying capacity and finally the effects of such behaviors on the whole structure. At the life-safety performance level, where the response of the structure is still away from collapse, a member failure criterion may be sufficient to constitute failure. In this paper, first the shear behavior of RC members is briefly discussed. Then, collecting experimental results of cyclic tests on RC columns, a probabilistic approach is utilized and new shear strength and deformation capacity models for RC columns that are susceptible to shear failure are developed and compared with available models.

¹ Assistant Professor, Northeastern University, Boston, USA. Email: Sasani@neu.edu

SHEAR BEHAVIOR OF RC MEMBERS

Shear transfer mechanisms and modes of failure of RC members

In a RC member under shear force, V , bending moment, M , and axial load, P , as shown in Figure 1 the shear force could be resisted by the forces supplied by: the compressive zone, V_{cz} ; the transverse component of aggregate interlock (interface) shear force at the crack, V_{aT} ; the dowel action of the flexural tensile reinforcement, V_d ; and the transverse reinforcement, V_s . Another mechanism of transferring the shear force is the arch (strut) action. Along with the beam action, arch (strut) action can participate in transferring some portion of the lateral load to the support. As a result, some portion of V_{cz} may be caused by the transverse component of arch (strut) action. Note that for short members, say with ratio of shear span to the section depth, a/h less than about 2.5, the arch (strut) action could make a significant contribution to the shear transfer mechanism.

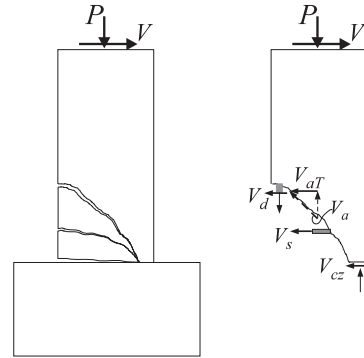


Figure 1. Shear transfer mechanisms

After the formation of inclined cracks and at loads near the failure of RC members with rectangular sections and without transverse reinforcement, depending on the shape and the nature of the cracks, the contribution of different mechanisms in shear carrying capacity could be as follows: 20%-40% by the compressive zone, V_{cz} , 33%-50% of the shear force could be carried by the aggregate interlock (interface) shear transfer, V_a , and 15%-25% by the dowel action, V_d , (ASCE-ACI-426 [1]). In RC members with transverse reinforcement, in addition to the above mechanisms, after the formation of inclined cracks, some portion of the shear is transferred by the transverse reinforcement. The presence of the transverse reinforcement can modify some of the shear transfer mechanisms discussed above. The transverse reinforcement restricts the width of diagonal tension cracks, which in turn improves the aggregate interlock shear transfer mechanism. By providing lateral supports for longitudinal reinforcement, particularly when the hoops are closely spaced or happen to be close to the bottom of the diagonal cracks and averting the dowel splitting cracks, the transverse reinforcement improves the dowel action. In addition to these effects, the confining effect of the transverse reinforcement improves the behavior of compressive struts (particularly under cyclic loading and after formation of intersecting diagonal cracks which will be discussed later in this chapter).

Under monotonically increasing lateral load, three basic modes of shear failure could be observed. As shown in Figure 2 the failure may be of shear-tension type (a) in which, soon after the formation of a major inclined flexural-shear crack (a crack that is initiated by flexure and is extended mainly by the shear force), the redistribution of the internal forces is not possible and sudden failure occurs. However, if the redistribution of the internal forces would be possible, the shear-compression failure (b) could occur which compared to mode (a) is less brittle. After the formation of the flexural-shear cracks, as a result of high tensile stress in the flexural reinforcement and the dowel action the shear-bond failure could occur (c). It should be noted that these three modes of failure could occur in RC members with and without transverse reinforcement.

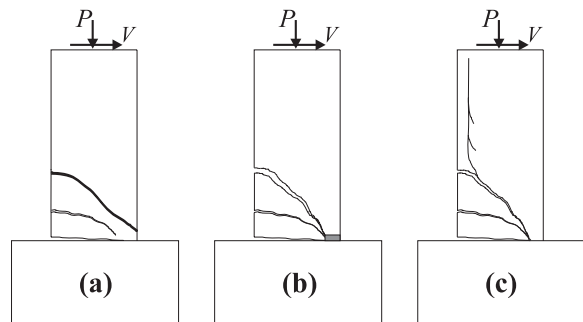


Figure 2. Common modes of shear failure: (a) shear-tension failure; (b) shear-compression failure; and (c) shear-bond failure.

Under cyclic loading (displacement) the shear transfer mechanisms and modes of failure are more complex. Although the preceding failure modes for monotonic loading also apply under cyclic loading, other modes of failure can occur under cyclic loading. One type of intersection shear-flexural crack is shown in Figure 3, in which the right hand side figure is of the specimen 00.105, tested by Wight [2]. The failure could occur between the adjacent stirrups, and usually occurs under a low level of axial compression, where upon reversal of loading, previously formed shear-flexural cracks on one side of the member could remain open, while cracks on the other side are opening as well. As a result, in the region in which the aggregate interlock shear transfer mechanism is weakened, the compressive concrete zone practically disappears and the dowel action becomes the main source of resisting shear force.

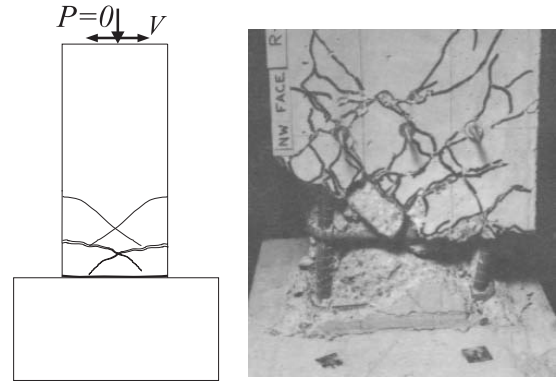


Figure 3. Intersecting shear-flexural cracks

Change in shear transfer mechanisms

Under monotonically increasing displacement, the relative contribution of different shear transfer mechanisms may change. Figure 4 shows the contribution of different internal shear force components in shear resistance of a RC member that failed in shear before yielding of flexural reinforcement (modified from ACI-ASCE-426 [1]). Note that the contribution is given at the crack. As shown in the figure, prior to flexural cracking the entire shear is carried by the uncracked concrete. Also prior to formation of inclined cracks, virtually no shear is transferred by transverse reinforcement. After yielding of the stirrups, the added shear has to be carried by other shear resisting mechanisms. As the inclined crack widens, the interface shear (aggregate interlock) decreases and eventually the RC member fails either by splitting (dowel) failure or as a result of failure of compressive zone due to combined shear and axial stresses.

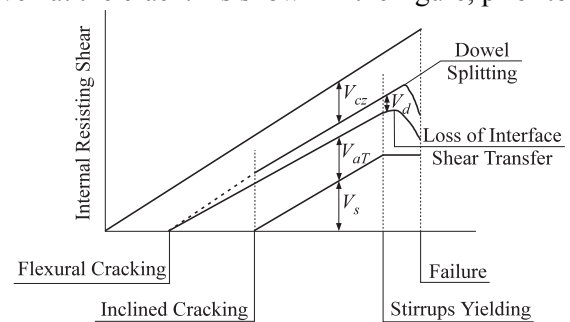


Figure 4. Distribution of internal shear forces

Another change in shear transfer mechanism of a RC member, which failed in shear after yielding of flexural reinforcement, is discussed by Wight and Sozen [2]. As shown in Figure 5 prior to the formation of inclined cracks, point A, no shear is transferred by transverse reinforcement and, after formation of inclined cracks, practically all the additional shear is carried by the transverse reinforcement. Point B shows the yielding of flexural reinforcement. At point C, the compressive concrete in the extreme fiber starts to exhibit longitudinal cracks and spalling of cover concrete starts and the cover concrete loses not only its axial carrying capacity, but also its shear resistance. Therefore, the demand on the hoops increases until they yield, point D. Beyond this point, there may still be some increase in the shear resisting force of the RC element or shear strength may drop. It should be noted that even though the shear strength increased somewhat beyond point D, since the yielding transverse reinforcement keeps elongating independent of the

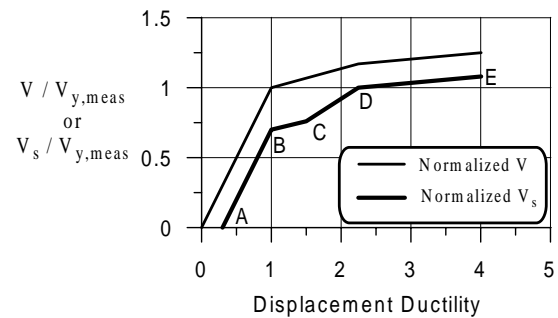


Figure 5. Change in shear transferred by transverse reinforcement

direction imposed displacement, under cyclic displacement the core concrete starts to segregate and the RC member may fail in shear-compression after a few cycles.

SHEAR STRENGTH CAPACITY MODEL FOR RC COLUMNS

Utilizing available experimental data on cyclic response of RC columns and making use of shear transfer mechanisms, a new model for estimating the shear strength capacity of RC columns is developed in this section. At the end, using the same set of test results, the reliabilities of currently used equations for shear strength of columns under seismic loading are examined.

Available experimental results

The Bayesian parameter estimation technique is used to fully utilize the available experimental data. Details of the Bayesian technique can be found in Box and Tiao [3], and Der Kiureghian [4]. In the Bayesian technique, one can make use of all available data. Therefore, not only the experimental results of RC members that failed in shear but also the test results of the ones that did not fail in shear are informative and will be used. In selecting experimental results only rectangular RC members with minimum dimensions of 150mm are considered. Also the minimum size for the flexural reinforcement bars is set equal to #4, i.e. a minimum diameter of about 13mm. Columns having concrete compressive strength, f'_c , between 17MPa and 45MPa are considered. The main criteria for identifying if a RC columns have failed in shear, is based on the classification of the shear failure mode done by the researchers who conducted the tests. In the absence of failure classification by the researchers, clear shear cracks observed in the pictures of the failed specimens are used to justify shear failure as the governing mode of failure. RC columns that did not fail in shear are the ones that either failed in bending or did not fail at all. All test members considered have symmetric reinforcement details about their main axis of the section. Because of the limited number of cyclic shear tests on RC columns under axial tension, columns under tension, in spite of their importance, are not considered in this study. Since a shear failure mode involving bond failure may be considered different from other types of shear failure, tested columns in which shear-bond failures were observed are not considered in this study.

Table 1 lists the columns used in this study and their references. Columns numbered 1 to 63 failed in shear and the remaining columns (columns numbered 64 to 89) did not fail in shear. Figure 6 shows the different types of test setups specified in Table 1. Note that for tests reported in [2], the test setups are considered as cantilevers. The experimental data was obtained from the database compiled by Eberhard [24] and from other references that are cited in this paper.

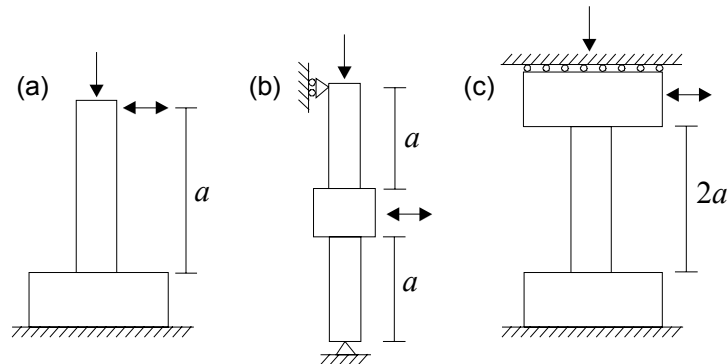


Figure 6. Test setups: (a) cantilever ; (b) double ended ; and (c) double curvature

The main characteristics of the specimens are shown in Figure 7. Note that the displacement ductility, μ , of a RC column is defined as the maximum displacement divided by the yield displacement.

Table 1. Test Specimens

No.	Specimen	Reference	<i>b</i>	<i>h</i>	Setu	No.	Specimen	Reference	<i>b</i>	<i>h</i>	Setu
1	6701	Endo, 1967 ^[5]	200	200	DE	51	OA2	Arakawa, 1989 ^[13]	180	180	DC
2	6703	Endo, 1967 ^[5]	200	200	DE	52	OA5	Arakawa, 1989 ^[13]	180	180	DC
3	6709	Endo, 1967 ^[5]	200	200	DE	53	CA025C	Ono, 1989 ^[14]	200	200	DC
4	6710	Endo, 1967 ^[5]	200	200	DE	54	U1	Saatcioglu, 1989 ^[15]	350	350	C
5	H1	Ikeda, 1968 ^[6]	200	200	DE	55	U2	Saatcioglu, 1989 ^[15]	350	350	C
6	H2	Ikeda, 1968 ^[6]	200	200	DE	56	3CLH18	Lynn, 1996 ^[16]	457	457	DC
7	H3	Ikeda, 1968 ^[6]	200	200	DE	57	2CLH18	Lynn, 1996 ^[16]	457	457	DC
8	H4	Ikeda, 1968 ^[6]	200	200	DE	58	2CMH18	Lynn, 1996 ^[16]	457	457	DC
9	H5	Ikeda, 1968 ^[6]	200	200	DE	59	3CMH18	Lynn, 1996 ^[16]	457	457	DC
10	O5	Ikeda, 1968 ^[6]	200	200	DE	60	3CMD12	Lynn, 1996 ^[16]	457	457	DC
11	40.033E	Wight, 1973 ^[2]	152	305	C	61	SC9	Aboutaha, 1999 ^[17]	457	914	C
12	40.033W	Wight, 1973 ^[2]	152	305	C	62	1	Sezen, 2002 ^[18]	457	457	DC
13	25.033E	Wight, 1973 ^[2]	152	305	C	63	2	Sezen, 2002 ^[18]	457	457	DC
14	25.033W	Wight, 1973 ^[2]	152	305	C						
15	00.033E	Wight, 1973 ^[2]	152	305	C	64	6705	Endo, 1967 ^[5]	200	200	DE
16	00.033W	Wight, 1973 ^[2]	152	305	C	65	6706	Endo, 1967 ^[5]	200	200	DE
17	40.048E	Wight, 1973 ^[2]	152	305	C	66	6707	Endo, 1967 ^[5]	200	200	DE
18	40.048W	Wight, 1973 ^[2]	152	305	C	67	6708	Endo, 1967 ^[5]	200	200	DE
19	00.048E	Wight, 1973 ^[2]	152	305	C	68	H9	Ikeda, 1968 ^[6]	200	200	DE
20	00.048W	Wight, 1973 ^[2]	152	305	C	69	H11	Ikeda, 1968 ^[6]	200	200	DE
21	40.067E	Wight, 1973 ^[2]	152	305	C	70	H13	Ikeda, 1968 ^[6]	200	200	DE
22	40.067W	Wight, 1973 ^[2]	152	305	C	71	H14	Ikeda, 1968 ^[6]	200	200	DE
23	00.067E	Wight, 1973 ^[2]	152	305	C	72	H15	Ikeda, 1968 ^[6]	200	200	DE
24	00.067W	Wight, 1973 ^[2]	152	305	C	73	H17	Ikeda, 1968 ^[6]	200	200	DE
25	40.092E	Wight, 1973 ^[2]	152	305	C	74	O1	Ikeda, 1968 ^[6]	200	200	DE
26	40.092W	Wight, 1973 ^[2]	152	305	C	75	O3	Ikeda, 1968 ^[6]	200	200	DE
27	00.105E	Wight, 1973 ^[2]	152	305	C	76	SP1	Gill, 1979 ^[19]	550	550	DE
28	00.105W	Wight, 1973 ^[2]	152	305	C	77	SP2	Gill, 1979 ^[19]	550	550	DE
29	120C-U	Ramirez, 1980 ^[7]	305	305	DC	78	SP3	Gill, 1979 ^[19]	550	550	DE
30	CUW	Umehara, 1982 ^[8]	410	230	DC	79	SP4	Gill, 1979 ^[19]	550	550	DE
31	CUS	Umehara, 1982 ^[8]	230	410	DC	80	3	Ghee, 1981 ^[20]	400	400	DE
32	2CUS	Umehara, 1982 ^[8]	230	410	DC	81	4	Ghee, 1981 ^[20]	400	400	DE
33	2D16RS	Ohue, 1985 ^[9]	200	200	DC	82	1	Soesianawati, 1986 ^[21]	400	400	DE
34	4D13RS	Ohue, 1985 ^[9]	200	200	DC	83	4	Soesianawati, 1986 ^[21]	400	400	DE
35	1-2	Toyoda, 1985 ^[10]	150	200	C	84	5	Watson, 1989 ^[22]	400	400	DE
36	1-6	Toyoda, 1985 ^[10]	150	200	C	85	6	Watson, 1989 ^[22]	400	400	DE
37	1-7	Toyoda, 1985 ^[10]	150	200	C	86	1	Tanaka, 1990 ^[23]	400	400	DE
38	1-9	Toyoda, 1985 ^[10]	150	200	C	87	2	Tanaka, 1990 ^[23]	400	400	DE
39	1-11	Toyoda, 1985 ^[10]	150	200	C	88	5	Tanaka, 1990 ^[23]	550	550	C
40	1-13	Toyoda, 1985 ^[10]	150	200	C	89	7	Tanaka, 1990 ^[23]	550	550	C
41	1-14	Toyoda, 1985 ^[10]	150	200	C						
42	1-15	Toyoda, 1985 ^[10]	150	200	C						
43	1	Imai, 1986 ^[11]	400	500	DC						
44	2-1	Machida, 1987 ^[12]	150	200	C						
45	2-2	Machida, 1987 ^[12]	150	200	C						
46	2-3	Machida, 1987 ^[12]	150	200	C						
47	2-4	Machida, 1987 ^[12]	150	200	C						
48	2-5	Machida, 1987 ^[12]	150	200	C						
49	2-9	Machida, 1987 ^[12]	150	200	C						
50	2-11	Machida, 1987 ^[12]	150	200	C						

(1) Test setup: C=cantilever; DC=double curvature; and DE=double ended

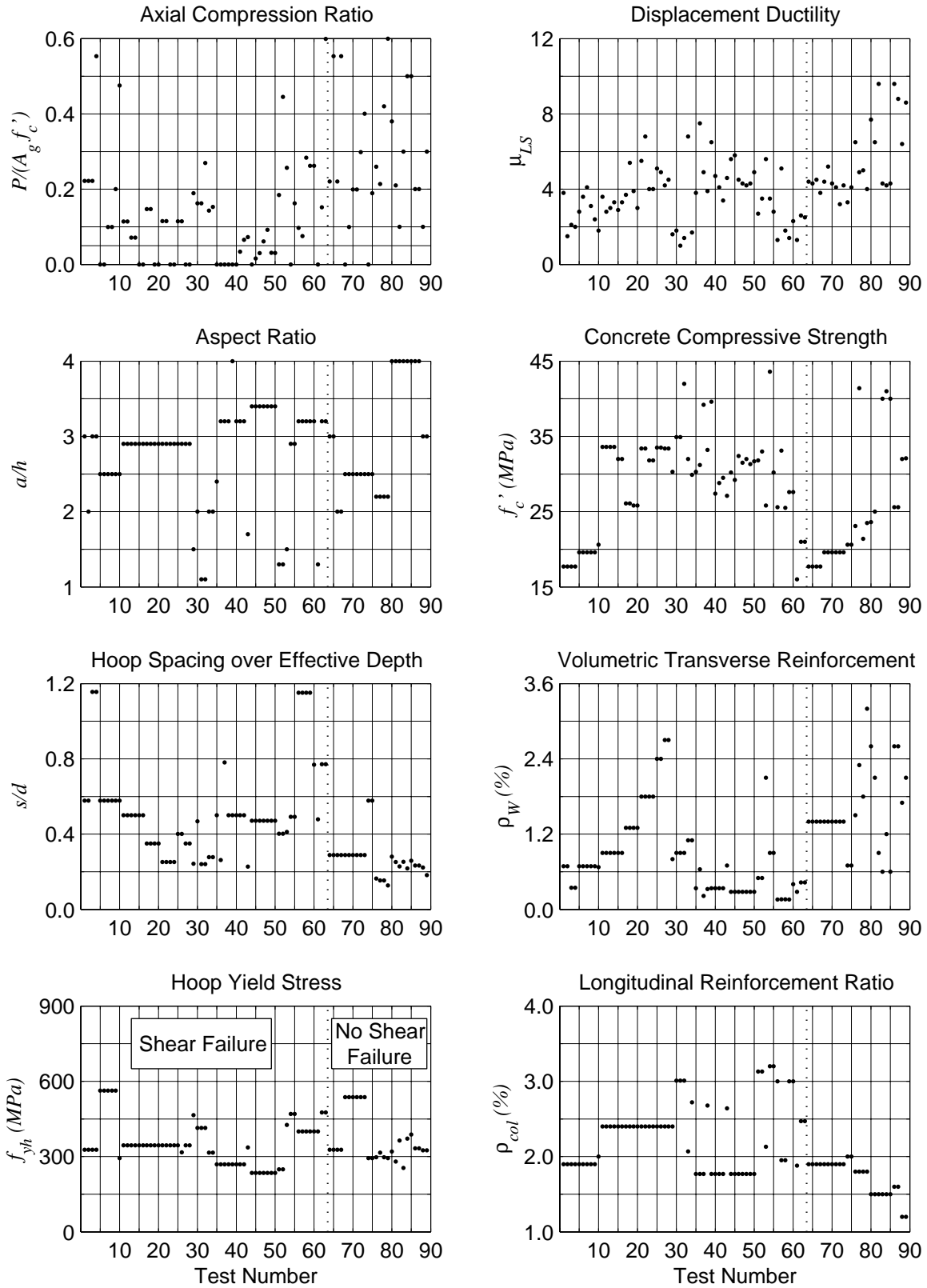


Figure 7. Main characteristics of test specimens

Proposed model for shear force capacity of RC columns

The shear strength of a RC member depends on many parameters, where the significant ones are:

Concrete strength affects the shear strength capacity of RC columns. The strength can include the tensile strength, the shear strength along shear-flexural cracks, the shear strength in the presence of compression stress (in the compression zone), and the compressive strength of the arch (strut) mechanism. In a simple model, it can be assumed that the shear strength of a RC column could be modeled as being proportional to $\sqrt{f'_c}bd$. The arch (strut) action is accounted for separately.

Arch (strut) action is important when the aspect ratio (a/h) is small. Based on test results by Kani [25], a decrease of the aspect ratio (a/h) from 2.5 to 1.5 may result in a minimum increase of 50% in the shear strength of a RC member without transverse reinforcement. Although even higher increase in shear strength is observed by Kani [25], ACI-318-02 [26] considers much lower increase in shear strength as the aspect ratio becomes smaller. In the model proposed here the effect of arch action on the shear strength capacity of RC columns is explicitly accounted for.

Axial load affects the shear strength of RC columns. Generally speaking, the presence of axial compression below some limits, increases the concrete shear strength. Axial compression not only increases the depth of the compressive zone and in turn its contribution to the shear capacity, but also limits the crack width in the tensile zone of a RC column which results in a more effective aggregate interlock (interface) shear mechanism.

Displacement ductility as a measure of the width of the shear-flexural cracks affects the shear strength of RC columns. As the displacement ductility increases, shear-flexural cracks open and the effectiveness of aggregate interlock shear transfer mechanism reduces. Figure 8 shows that beyond a displacement ductility of about two, by increasing the displacement ductility, the shear deformation increases approximately linearly. This may be explained by the fact that by increasing the displacement ductility, the shear transferred through the aggregate interlock mechanism drops. Although the effect of displacement ductility on the shear transfer through the compressive zone may be different, for simplicity in this study it is assumed that the shear strength of the concrete section reduces linearly as the displacement ductility increases.

One may use the maximum displacement, instead of the ductility, as a measure of reduction in shear strength of RC members, in which case there will be no need to find the yield displacement. However, since the maximum displacement is affected by the flexibility of the member, which in turn has little bearing on the shear strength deterioration, the displacement ductility seems to be a better measure of shear deterioration.

Transverse reinforcement is assumed to provide a shear strength proportional to that given by a truss analogy.

Longitudinal reinforcement ratio and dowel action are not considered in the proposed shear model and their effects will be discussed later on.

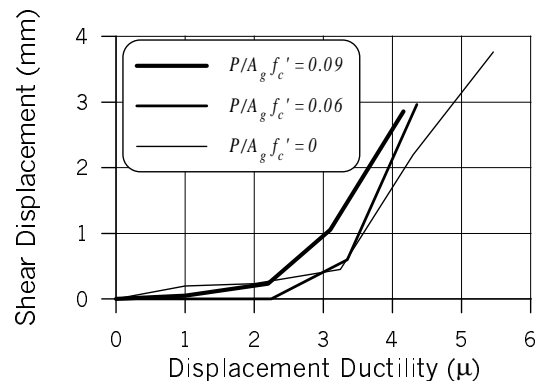


Figure 8. Effect of displacement ductility on shear displacement (Machida [12])

Seismic performance level and imposed force-displacement history need to be specified to define the shear strength of RC members. For instance at the life safety performance level (LSPL), one may limit the reduction in the lateral load carrying capacity of a RC member as a means to control the imposed damage to the member. Furthermore, under random types of ground motions, the RC member may experience few cycles of large lateral displacement and one needs to make sure that the response of the member under such an action is stable. Therefore, the shear strength and the corresponding displacement ductility of a RC column at the LSPL under random type of ground motion is defined as shown in Figure 9. A force-displacement cycle with less than 20% drop in shear carrying capacity is called a stable cycle. Note that the shear force reduction as a result of $P-\Delta$ is excluded, because it is not related to shear strength reduction of the member. The maximum displacement at which there are at least two full stable cycles of force-displacement loops, excluding the $P-\Delta$ effect, is defined as the displacement capacity corresponding to the shear force capacity. If at some force-displacement loop level there are less than two stable cycles, the displacement capacity is found by linear interpolation between the largest displacement with at least two stable cycles and a larger displacement with less than two stable cycles, based on the number of available stable cycles in the latter one. In Figure 9 there is only one stable cycle at the largest displacement, therefore, Δ_{max} is set equal to the average of the maximum displacement of the last cycle and that of the previous one.

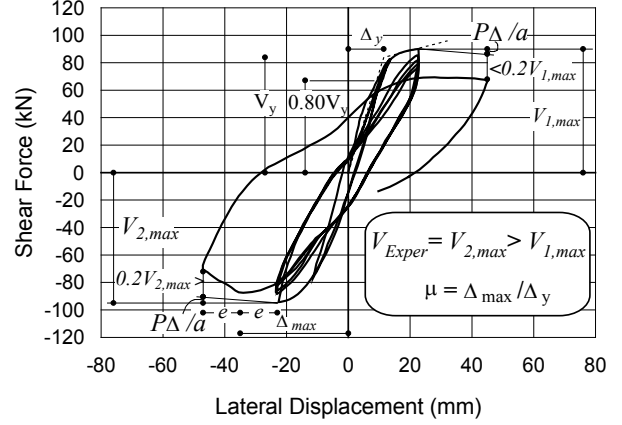


Figure 9. Experimental shear strength and corresponding displacement ductility

Proposed Model

Considering parameters that affect the shear strength capacity of RC columns as discussed in the previous section and modifying available shear strength models

$$\left\{ \begin{array}{l} \hat{V}_c = \alpha_1 \left[a_{asp} (1 - \alpha_2 \mu) + \alpha_3 \frac{P}{A_g f'_c} \right] \sqrt{f'_c f_{ss}} b d + \alpha_4 \frac{A_{sh} f_{yh} d}{s} \\ a_{asp} = \left(\alpha_5 - \frac{M}{Vh} \right) \geq 1 \quad \text{and} \quad \text{If } \frac{P}{A_g f'_c} > \alpha_6 \Rightarrow \frac{P}{A_g f'_c} = \alpha_6 \end{array} \right. \quad (1)$$

is proposed for estimating the shear strength of RC columns, \hat{V}_c . The superposed hat on V_c is used to emphasize that the model is not exact and is subject to error. f_{ss} is a scaling stress equal to 1 MPa (or its equivalent in other unit systems) and is used to make the parameters of the model dimensionless. Note that a is replaced by a more general term of M/V . There are six unknown parameters ($\alpha_1, \alpha_2, \alpha_3, \alpha_4, \alpha_5, \alpha_6$) in the model. Note that α_4 is included in the model to examine the truss model assumption. The statistics of the parameters are found using the Bayesian parameter estimation technique. In order to account for the error in (1), after proper transformation, the shear strength capacity can be found from

$$V_c = e^{\varepsilon_v} \hat{V}_c \quad (2)$$

where ε_v is the model error which has normal distribution with zero mean and standard deviation σ_v . The mean value of σ_v is found equal to 0.14 and the mean values of the parameters are given in (3)

$$\left\{ \begin{array}{l} \bar{V}_c = 0.22 \left[a_{asp} (1 - 0.08\mu) + 2.9 \frac{P}{A_g f'_c} \right] \sqrt{f'_c f_{ss}} bd + \frac{2}{3} \frac{A_{sh} f_{yh} d}{s} \\ a_{asp} = \left(3.7 - \frac{M}{Vh} \right) \geq 1 \quad \text{and} \quad \text{If } \frac{P}{A_g f'_c} > 0.42 \Rightarrow \frac{P}{A_g f'_c} = 0.42 \end{array} \right. \quad (3)$$

Figure 10 shows the relative error in predicting the shear strength capacity of the RC columns. The maximum relative error in predicting the shear strength of columns that failed in shear which are marked by circles is $\pm 27\%$. The columns that did not fail in shear which are marked by diamonds are supposed to be below the horizontal axis but some of them are above the axis which means that the behavior of such columns is not predicted well by the model.

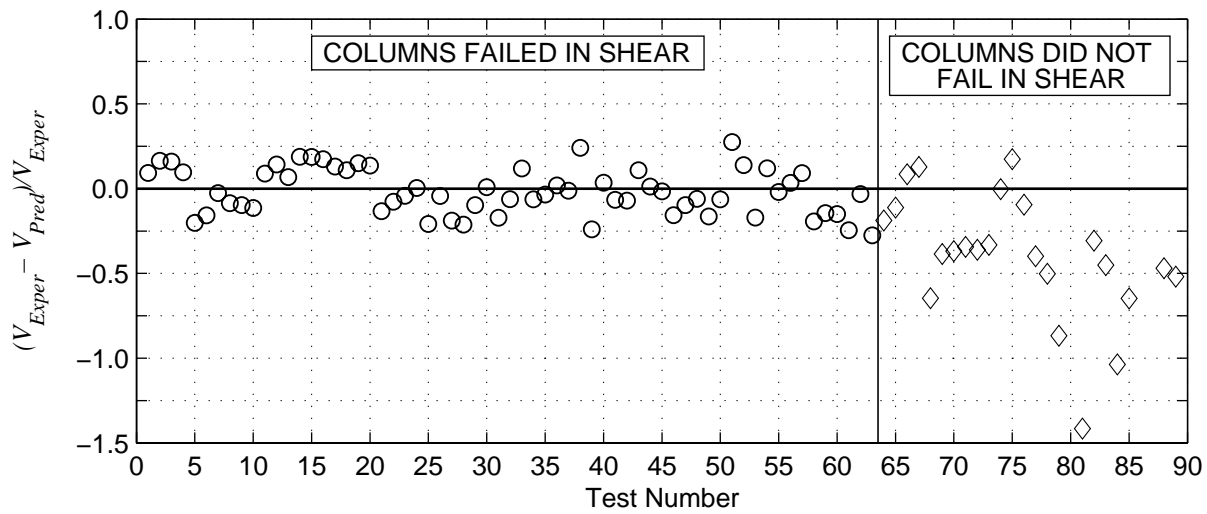


Figure 10. Error in shear prediction

Figure 11 compares the experimental and mean values of predicted shear strength capacities of RC columns. The 45 degree line represents a perfect correlation between the experimental and predicted shear strength capacities. As can be seen, the circles representing columns that failed in shear are located in the vicinity of the 45 degree line. For most of the columns that did not fail in shear, the predicted shear strength capacities are larger than those of the experimental values, as expected.

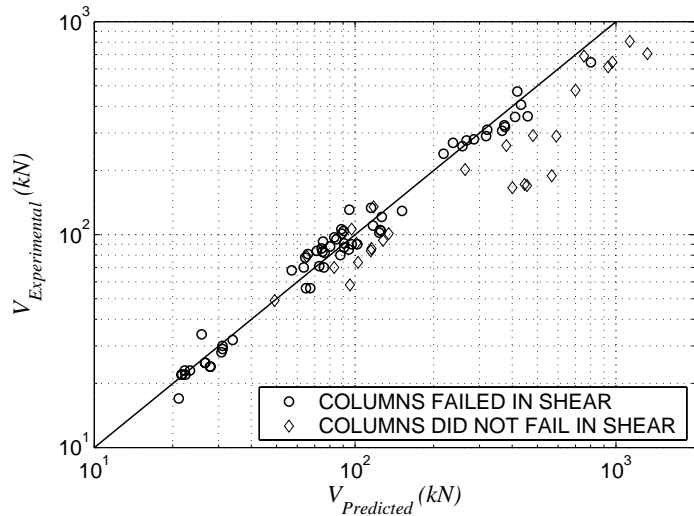


Figure 11. Experimental shear versus shear predicted

Figure 12 shows the relative error in calculating shear strength capacity of RC columns using, FEMA-356 [27], FEMA-273 [28], and ACI-318 [26]. Comparing the errors for estimating the shear strength capacity of the columns that failed in shear given in Figures 10 and 12, the significant improvement achieved through the proposed model becomes obvious.

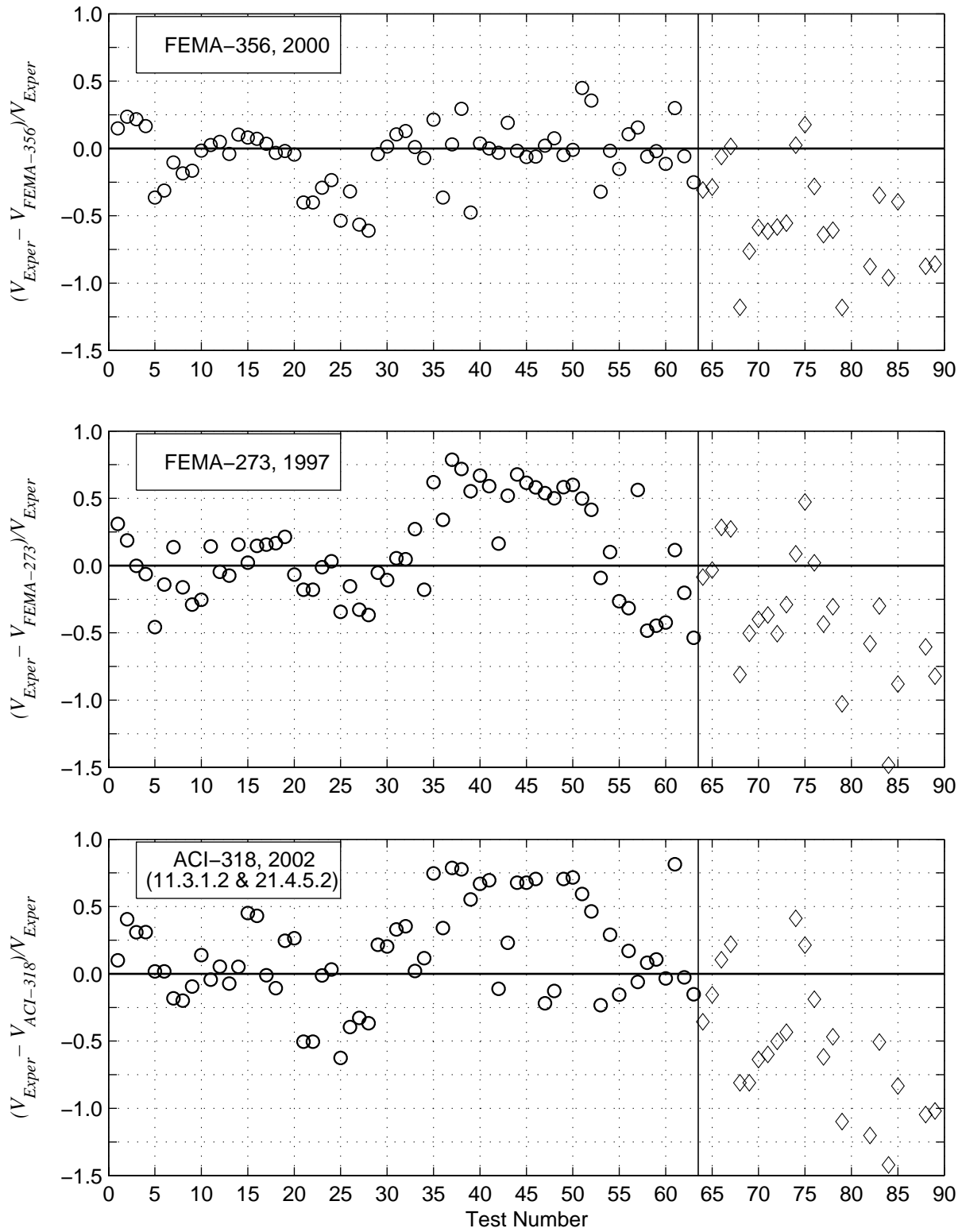


Figure 12. Relative error in shear strength estimation using, FEMA-356, FEMA-273, and ACI-318

DEFORMATION CAPACITY MODEL FOR RC COLUMNS

In this section a model is proposed for estimating the drift ratio capacity, DR_c , of RC elements. Drift ratio, DR , is defined as the lateral tip displacement divided by the length of the element.

Deformation of RC elements

Deformation of RC elements under lateral loads consists of flexural, bond slip, and shear components. The tip flexural displacement capacity, Δ_f , of a fixed base cantilever of length a , can be written as:

$$\Delta_f = \Delta_y + \Delta_p \quad (4)$$

where Δ_y and Δ_p are the yield displacement and plastic displacement, respectively. The plastic displacement can be found from (Paulay [29])

$$\Delta_p = \Phi_p L_p (a - L_p / 2) \quad (5)$$

where Φ_p is the maximum plastic curvature and L_p is the plastic hinge length. Given that the plastic hinge length is small compared to the length of RC elements, $(a - L_p / 2)$ in (5) can be approximated by a .

Therefore, from (4) and (5) we obtain

$$DR_f = DR_y + \Phi_p L_p \quad (6)$$

where DR_f and DR_y are the total flexural and yield drift ratios, respectively. Another source of deformation is the bond slip in the foundation and the resulting rotation at the base of the cantilever. One can account for the deformation due to the bond slip explicitly or by adjusting the plastic hinge length (Paulay [29]).

The drift ratio due to shear deformation (DR_s) of cracked RC elements can be calculated using the relationship proposed by Park [30]

$$DR_s = \left(\frac{1}{\rho_v} + 4n \right) \frac{V_s}{E_s b_w d} \quad (7)$$

where ρ_v is the shear reinforcement ratio, n is the ratio of modulus of elasticity of steel and concrete, V_s is the shear transferred through the truss action, E_s is the modulus of elasticity of steel, and b_w and d are the width of the web and the effective depth of the section, respectively.

Effects of different parameters on deformation capacity of RC elements

Main parameters affecting (6) are the amount and mechanical characteristics of transverse and longitudinal reinforcement, amount of axial force as well as geometric characteristics of elements. In Figure 13(a), data points connected by solid lines represent experimental results of specimens with similar characteristics but different amounts of volumetric transverse reinforcement, ρ_w , subjected to similar cyclic displacement histories. Note that the mode of failure for each specimen is identified. Similarly, Figure 13(b), (c) and (d) show the drift ratio capacity for specimens that differ only in η_0 , a/h , and, ρ_t , respectively. Effects of these parameters on deformation capacity of RC elements are examined below.

As can be seen in Figure 13 (a) for all the cases, an increase in the volumetric transverse reinforcement ρ_w results in a larger drift ratio capacity, DR_c . A larger ρ_w improves the flexural deformation capacity and delays shear failure of columns.

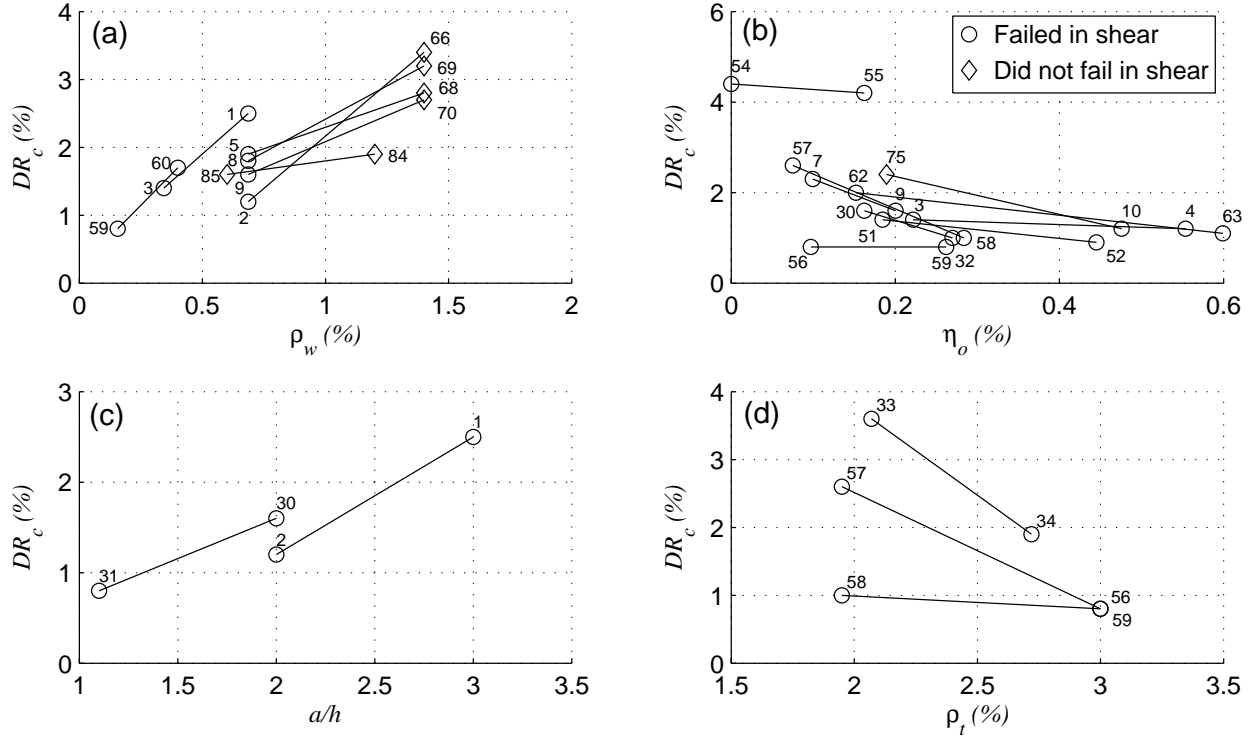


Figure 13. Effects of different parameters on drift capacity

Figure 13(b) shows the effect of axial load on drift ratio capacity. The amount of axial load directly affects the depth of the compressive zone and in turn the ultimate curvature of RC sections which affects the drift capacity of elements (see Equation 6). As it can be seen, in almost all cases larger values of η_0 results in smaller drift ratio capacity. Figure 13(c) shows the effect of a/h on drift ratio capacity. For both cases shown, an increase in the drift ratio capacity as a result of an increase in the aspect ratio is observed. Figure 13(d) shows the effect of longitudinal reinforcement ratio on drift ratio capacity. As it can be seen, increasing the longitudinal reinforcement results in smaller drift ratio capacity.

Drift ratio capacity model

For a cantilever having uniform section properties, the elastic flexural deformation under a tip lateral load can be calculated using a linear curvature distribution over the length of the element. However, in RC elements because of the formation of cracks, mainly at the vicinity of the base where the bending moment is maximum, there is a significant reduction in the flexural stiffness of sections in that region. As a result, the tip yield deformation is mainly due to curvature in the vicinity of the base. Therefore similar to plastic drift ratio, the yield drift ratio can be estimated from $DR_y = \Phi_y L_y$, where L_y is some portion of length of the element. Given that the ultimate curvature is $\Phi_u = \Phi_y + \Phi_p$, (6) can be rewritten as

$$DR_f = \Phi_u L_p^* \quad (8)$$

where L_p^* is a length that can be considered as a weighted average between L_p and L_y .

In order to develop a model that is not too complex yet can reliably estimate the drift capacity of RC elements that failed either in flexure or in shear, and given the fact that the shear deformation is a small portion of the total deformation, let us first examine (6). The ultimate curvature in (6) can be limited by the maximum concrete usable strain, which in turn is significantly affected by ρ_w . In other words, the larger the ρ_w , the larger the Φ_u becomes. Moreover, η_0 directly affects the depth of the compressive zone

and therefore affects the ultimate curvature. Therefore, one can assume that $\Phi_u \propto \rho_w^\alpha \eta_0^\gamma$, where α and γ are parameters. Similar to the plastic hinge length, L_p^* can be considered to be proportional to the shear span of elements (Paulay [29]). Given the facts that the test results indicate a direct relationship between a/h and the drift ratio capacity and the a/h can be used as a measure of the amount of shear force transferred to columns, it is decided to replace L_p^* with $\theta a/h$, where θ is a parameter having one value for cantilever elements and another value for double curvature and double-ended elements.

$$\hat{D}R_c = \theta \rho_w^\alpha \eta_0^\gamma \frac{a}{h} \quad (9)$$

The superposed hat on the drift ratio capacity signifies that the model is not exact and is subject to error. Figure 14 shows the concentration of deformation on one end of double curvature and double ended specimens. In such specimens, if damage is concentrated on one end, the drift capacity will be mainly due to the deformation on the damaged end. Therefore, compared to a similar cantilever specimen, the drift capacity is expected to be smaller. The parameter θ is included in the model to account for such a difference between cantilever specimens and double curvature and double ended specimens.

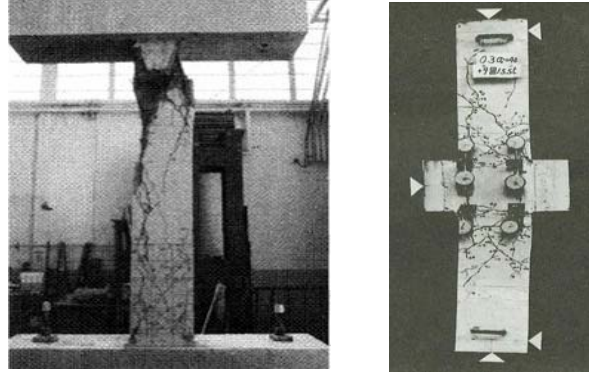


Figure 14. Concentration of deformation in top part of a double curvature specimen [31], left; and in bottom part of a double ended specimen [8], right.

The mean shear to total deformations of columns tested by Lynn [31] is about 18% (Bazan [32]). Because the contribution of the shear deformation in total deformation is not significant, the shear deformation is not explicitly accounted for in the model. However, as given in (7), ρ_w , (which is associated with ρ_v) and a/h (which affects the amount of shear force applied to the column) are used in (9) and therefore implicitly account for the shear deformation.

In order to account for the error in (9), after a proper transformation, we obtain

$$DR_c = e^{\varepsilon_{DR}} \hat{D}R_c \quad (10)$$

where ε_{DR} is the model error which has normal distribution with zero mean and standard deviation σ_{DR} . The Mean value of the parameters are given in (11),

$$\overline{DR}_c = \theta \rho_w^{0.77} \eta_0^{-0.18} \frac{a}{h} \quad (11)$$

where $\theta = 1.0$ for cantilever columns and $\theta = 0.85$ for double-curvature and double-ended columns. In addition to the parameters used in the model, limits are also imposed on ρ_w , η_0 , and a/d . For $\rho_w > 1.7\%$, use $\rho_w = 1.7\%$. Note that the smallest value of ρ_w used to develop the model is 0.16% and the model is not developed for columns without transverse reinforcement. Also, for $\eta_0 < 0.13$ use $\eta_0 = 0.13$. Imposing limits on a/d did not reduce the standard deviation of the error. Also note that the standard deviation of the error term is only $\sigma_{DR} = 0.22$. Note that the inclusion of the longitudinal reinforcement ratio in the model did not reduce the standard deviation of the error term. Figure 15 compares the experimental and mean predicted drift ratio capacities. As it can be seen, for columns that failed in shear, the circles are close to the 45 degree line. For columns that did not fail in shear, shown in diamonds, for most cases the predicted value is larger than the experimental value (as expected).

CONCLUSIONS

Experimental test results of 89 reinforced concrete (RC) columns and shear transfer mechanics of columns, as well as the mechanics of deformation of RC columns are used to develop new shear strength and drift ratio capacity models. It is shown that the proposed shear strength capacity model has a coefficient of variation of only 0.14 and can predict the shear strength of columns significantly better than equations available in current codes and standards. It is observed that better predictions of shear strength of columns are obtained, if about 2/3 of the strength provided by transverse reinforcement based on a simple truss model is considered effective.

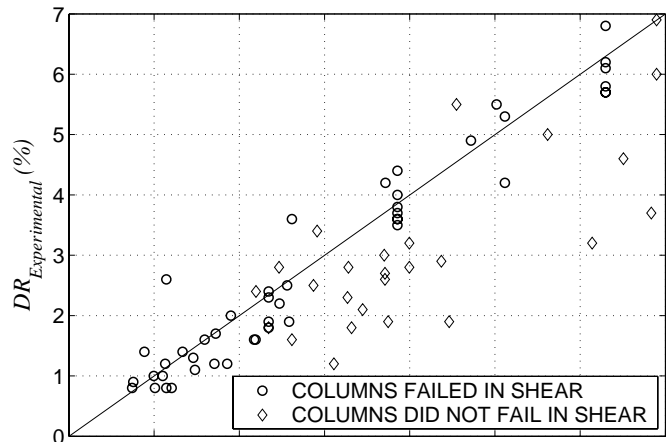


Figure 15. Comparison between experimental and predicted drift ratio capacities

In the drift ratio capacity model, the difference between the deformation of double curvature and double ended columns (in which damage can concentrate on one end of the specimen) and cantilever columns is accounted for. The coefficient of the variation of the drift capacity model is 0.22.

REFERENCES

1. ASCE-ACI-426. "The shear strength of reinforced concrete members: Chapter 1 to 4." Journal of Structural Engineering, ASCE, 1973; 99(6): 1091-1187.
2. Wight JK, Sozen MA. "Shear strength decay in reinforced concrete columns subjected to large deflection reversals." UIUL-ENG-73-2017 Report, University of Illinois, Illinois, 1973.
3. Box GEP, Tiao GC. "Bayesian inference in statistical analysis." Addison-Wesley, Reading, Massachusetts, 1992.
4. Der Kiureghian A. "A Bayesian framework for fragility assessment." Proceedings of the 8th International Conference On Applications of Statistics and Probability (ICASP) in Civil Engineering Reliability and Risk Analysis, Sydney, Australia, RE Melchers and MG Stewart, Eds., 1999; 2: 1003-1010.
5. Endo. "Test of reinforced concrete columns subjected to a constant axial load and lateral loads." Experimental Studies on Reinforced Concrete Members and Composites Steel and Reinforced Concrete Members. Edited by: Umemura H, Aoyama H, and Ito M. Japan, 1967: 1-16.
6. Ikeda A. "Experimental studies on load-deflection characteristics of reinforced concrete columns subjected to alternate loading." Report of the Training Institute for Engineering Teachers, Yokohama National University, Kanagawa, Japan, 1968.
7. Ramirez H, Jirsa JO. "Effect of axial load on shear behavior of short RC columns under cyclic Lateral deformations." PMFSEL Report No. 80-1, Phil M. Ferguson Structural Engineering Laboratory, University of Texas, Austin, Texas, 1980.
8. Umehara H, Jirsa JO. "Shear strength deterioration of short reinforced concrete columns under cyclic deformations." PMFSEL Report No. 82-3, Department of Civil Engineering, University of Texas at Austin, Austin, Texas, 1982.
9. Ohue M, Morimoto H, Fujii S, Morita S. "The behavior of RC short columns failing in splitting bond-shear under dynamic lateral loading." Transactions of the Japan Concrete Institute, 1985; 7: 293-300.

10. Toyoda K, Mutsuyoshi H, and Machida A. "Experimental study on evaluation of the ultimate deflection of reinforced concrete members." Transaction of the Japan Concrete Institute, 1985; 7: 535-542. (And Personal Communication with Mutsuyoshi, H.)
11. Imai H, Yamamoto Y. "A study on causes of earthquake damage of Izumi high school due to Miyagi-Ken-Oki Earthquake in 1978." Transactions of the Japan Concrete Institute, 1986; 8: 405-418.
12. Machida A, Mutsuyoshi H, Toyoda K. "Evaluation of ultimate deflection of reinforced concrete members." Concrete Library of JSCE, 1987; 10: 139-154.
13. Arakawa T, Arai Y, Mizoguchi M, Yoshida, M. "Shear resisting behavior of short reinforced concrete columns under biaxial bending-shear." Transactions of the Japan Concrete Institute, 1989; 11: 317-324.
14. Ono A, Shirai N, Adachi H, Sakamaki Y. "Elasto-plastic behavior of reinforced concrete columns with fluctuating axial force." Transactions of the Japan Concrete Institute, 1989; 11: 239-246.
15. Saatcioglu M, Ozcebe G. "Response of reinforced concrete columns to simulated seismic loading." ACI Structural Journal, 1989; 86(1):3-12
16. Lynn A, Moehle JP, Mahin SA, Holmes WT. "Seismic evaluation of existing reinforced concrete buildings columns." Earthquake Spectra, 1996; 12(4): 715-739.
17. Aboutaha RS, Engelhardt MD, Jirsa JO, Kreger ME. "Rehabilitation of shear critical concrete columns by use of rectangular steel jackets." ACI Structural Journal, 1999; 96(1): 68-78.
18. Sezen H, Moehle JP. "Seismic behavior of shear-critical reinforced concrete building columns." Proceedings of the 7th U.S. National Conference on Earthquake Engineering, Boston, Massachusetts, 2002. CD-Rom. Earthquake Engineering Research Institute.
19. Gill WD, Park R, Priestley MJN. "Ductility of rectangular reinforced concrete columns with axial load." Report 79-1, Department of Civil Engineering, University of Canterbury, New Zealand, 1979.
20. Ghee AB, Priestley MJN, Park R. "Ductility of reinforced bridge piers under seismic loading." Report 81-3, Department of Civil Engineering, University of Canterbury, New Zealand, 1981.
21. Soesianawati MT, Park R, Priestley MJN. "Limited ductility design of reinforced concrete columns." Report 86-10, Department of Civil Engineering, University of Canterbury, New Zealand, 1986.
22. Watson S, Park R. "Design of reinforced concrete frames of limited ductility." Report 89-4, Department of Civil Engineering, University of Canterbury, New Zealand, 1989.
23. Tanaka H, Park R. "Effect of lateral confinement reinforcement on the ductile behavior of reinforced concrete columns." Report 90-2, Department of Civil Engineering, University of Canterbury, New Zealand, 1990.
24. Eberhard M. "Structural performance database." <<http://maximus.ce.washington.edu/~peeral/>>. University of Washington, 2004.
25. Kani, GNJ. "Basic facts concerning shear failure." Journal of the American Concrete Institute, ACI, 1996; 63(6): 675-690.
26. ACI-318-02. Building code requirements for structural concrete and commentary. American Concrete Institute, Michigan, 2002.
27. FEMA-356. Prestandard and Commentary for the Seismic Rehabilitation of Buildings. Federal Emergency Management Agency, Washington, D.C., 2000.
28. FEMA-273. NEHRP Guidelines for the Seismic Rehabilitation of Buildings. Building Seismic Safety Council, Washington, D.C., 1997.
29. Paulay T, Priestley MJN. "Seismic design of reinforced concrete and masonry buildings." John Wiley & Sons, 1992.
30. Park R, Paulay T. "Reinforced Concrete Structures." Wiley-Interscience, John Wiley & Sons, New York, 1975.
31. Lynn A. "Seismic evaluation of existing reinforced concrete building columns." PhD thesis, University of California at Berkeley, California, 2001.
32. Bazan M, Sasani M. "A new damage model for reinforced concrete elements." Proceedings of the 13th World Conference on Earthquake Engineering, Vancouver, B.C., Canada, 2004: Paper No. 2846.